



## RESEARCH ARTICLE

WILEY

# 3D geometric survey of cultural heritage by UAV in inaccessible coastal or shallow aquatic environments

Mariluz Gil-Docampo<sup>1</sup>  | Simón Peña-Villasenín<sup>1,2</sup>  | Ana M. S. Bettencourt<sup>2</sup> | Juan Ortiz-Sanz<sup>1</sup> | Sara Peraleda-Vázquez<sup>1</sup>

<sup>1</sup>Agroforestry Engineering Department, University of Santiago de Compostela, Higher Polytechnic School of Engineering, Lugo, Spain

<sup>2</sup>Landscapes, Heritage and Territory Laboratory (Lab2PT); History Department, University of Minho, Braga, Portugal

## Correspondence

Simón Peña-Villasenín, Agroforestry Engineering Department, University of Santiago de Compostela, Higher Polytechnic School of Engineering, Lugo, Spain.  
Email: [simon.pena@rai.usc.es](mailto:simon.pena@rai.usc.es)

## Funding information

Xunta de Galicia

## Abstract

Cultural heritage in coastal or shallow aquatic environments is often located in areas where access is difficult or where accurate survey and documentation may not always be possible with terrestrial or aquatic equipment. The combination of photogrammetry and unmanned aerial vehicles (UAVs) generates a range of possibilities across multiple sectors, including history, ethnography and cultural heritage studies. Additionally, these methods can be used to prospect new archaeological sites. This article presents three case studies that use UAV techniques and Structure from Motion and Multiview Stereo (SfM-MVS) photogrammetry to conduct topographic and geometric registrations of archaeological, historical and ethnographic sites (some of which are classified as cultural heritage sites). These examples are located in coastal or shallow aquatic environments that are difficult to survey with traditional methods. The results show that it is possible to carry out detailed geometric registration and heritage prospection over large coastal or shallow aquatic environments using a low-cost UAV. Furthermore, the results of this work show great advantages in terms of cost and quality, even in cases where the seabed is below a shallow water column. Other particularities of SfM-MVS application in aquatic environments are discussed. From an interdisciplinary perspective, this methodology will offer new possibilities for the study, restoration and conservation of archaeological, historical and ethnographic monuments.

## KEYWORDS

3D modelling, aerial prospecting, close-range photogrammetry, cultural heritage

## 1 | INTRODUCTION

A thorough examination of the visual, spatial and topographic records is critical for ensuring the accurate study, conservation and dissemination of cultural heritage archived within coastal or shallow aquatic environments. The traditional methodologies used for these

examinations have been partially replaced in recent decades by large data acquisition techniques such as terrestrial laser scanning (TLS) (Brumana et al., 2014; Guarnieri et al., 2013) or Structure from Motion and Multiview Stereo (SfM-MVS) photogrammetry (Ortiz-Sanz et al., 2013; Santagati et al., 2013). These technologies allow for the generation of a high-resolution, 3D photorealistic depiction of a

This is an open access article under the terms of the [Creative Commons Attribution-NonCommercial-NoDerivs](https://creativecommons.org/licenses/by-nc-nd/4.0/) License, which permits use and distribution in any medium, provided the original work is properly cited, the use is non-commercial and no modifications or adaptations are made.

© 2023 The Authors. *Archaeological Prospection* published by John Wiley & Sons Ltd.

location or feature and provide more complete and rigorous geometric documentation of heritage remains than can otherwise be obtained by traditional techniques. Additionally, these methods favour greater objectivity in the scientific-technical study and are a more attractive form of disseminating cultural heritage to the general public while also providing for more agile and efficient surveying (Aicardi et al., 2018; Dong et al., 2020). Although both TLS and SfM-MVS photogrammetry are the primary techniques used for 3D heritage registration, SfM-MVS has become more commonly used than TLS due to its low cost and feasibility and shows great potential in a variety of tasks related to the geometric registration of cultural heritage sites (Peña-Villasenín et al., 2017, 2020). Photogrammetry has a long history and has undergone important advancements with the introduction of SfM-MVS approaches (Remondino & El-Hakim, 2006; Snavely et al., 2006; Westoby et al., 2012). These methodologies are even more relevant in studies of rock art due to their noninvasive nature and the possibility of applying 3D rendering posttreatments, which allow documenting these heritage elements in an objective way (Gil-Docampo et al., 2019; Peña-Villasenín et al., 2019; Santos-Estevez et al., 2020).

### 1.1 | SfM-MVS photogrammetry

The SfM-MVS process is divided into three main phases. First, an internal and external orientation of the images is performed. During this step, camera position and scene geometry are reconstructed simultaneously through the automatic identification of matching features by the scale invariant feature transform (SIFT) method (Chandran et al., 1997; Lowe, 1999; Lowe, 2004). These features enable initial estimations of camera positions and object coordinates, which are then iteratively refined using nonlinear least-squares minimization. The sparse bundle-adjustment system ‘Bundler’ (Snavely et al., 2008) is used for this task. Second, an enhanced-density point cloud and a 3D mesh can be derived using the clustering view for multiview stereo (CMVS) algorithm and the patch-based multiview stereo (PMVS2) algorithm (Furukawa et al., 2010; Furukawa & Ponce, 2010). Once the densified point cloud is obtained, it can be used to generate 3D models, digital elevation models (DEMs), nadir and side view orthomosaics and planimetric vectorizations of the study elements. Regarding photographic capture, numerous studies and documentation from photogrammetric software developers provide standardized guidance on the spatial distributions of photographic capture for SfM-MVS photogrammetry (Agüera-Vega et al., 2017; Martínez et al., 2013; Pepe & Costantino, 2020; Remondino et al., 2011; Remondino & El-Hakim, 2006).

### 1.2 | Documenting aquatic cultural heritage with UAVs and SfM-MVS

It is often difficult to access heritage sites in coastal or shallow aquatic environments. Photogrammetry has shown great potential for registering a variety of cultural heritage elements. However, in inaccessible

coastal or shallow aquatic environments, its application is difficult, and the archaeological prospection and geometric and topographic registration may be complicated by issues of accessibility. Therefore, geometric image registration is not always possible despite access to terrestrial or aquatic equipment, which results in an incomplete study.

Simultaneous with the evolution of photogrammetry, there was an expansion in the civil applications of unmanned aerial vehicles (UAVs). Its ability to carry a wide variety of sensors allows multiple applications, such as acquiring images at low altitudes for 3D modelling of heritage sites or obtaining a geometric or topographic terrain record (Heincke et al., 2019; Themistocleous, 2020). The ease of use and quality of the results obtained currently make UAVs a common tool in cultural heritage research. SfM-MVS photogrammetry and UAVs generate a range of possibilities that, in many cases, remain to be explored. UAVs can be used for taking photographs in inaccessible areas or for aerial prospection over large terrains. The combination of SfM-MVS photogrammetry and UAVs can reduce the problems associated with prospecting and registering cultural features archived in inaccessible coastal or shallow aquatic environments.

The development and optimization of work protocols with SfM-MVS photogrammetry can have a considerable social and scientific impact because these techniques improve the quantity and quality of heritage records in inaccessible areas. The main objective of this study is to show how the integration of UAVs and SfM-MVS photogrammetry is capable of prospecting and geometrically documenting various examples of historic, ethnographic and rock art sites located in places that are difficult to access, such as shallow aquatic environments, intertidal zones or coastal areas. The case studies involve three areas of interest: (1) the remains of salt flats and associated tide mills; (2) the archaeological remains of a Roman bridge with evidence of fishery activities and weirs; and (3) coastal rock art.

## 2 | MATERIALS AND METHODS

This section describes the case studies and the main methodologies and equipment used for the field survey, processing work, and the exporting and publishing of the results.

### 2.1 | Study cases

All case studies are located in the northwestern Iberian Peninsula (Figure 1). The chosen locations encompass several common heritage typologies located in coastal, intertidal or shallow aquatic environments. The main characteristics of the three case studies are presented below.

#### 2.1.1 | Case 1. Tide mill and Ulló saline, Vilaboa, Spain

Case 1 (Figure 2a) was a salt mining area with a tide mill and a long history of occupation. It is located in the innermost area of the Vigo

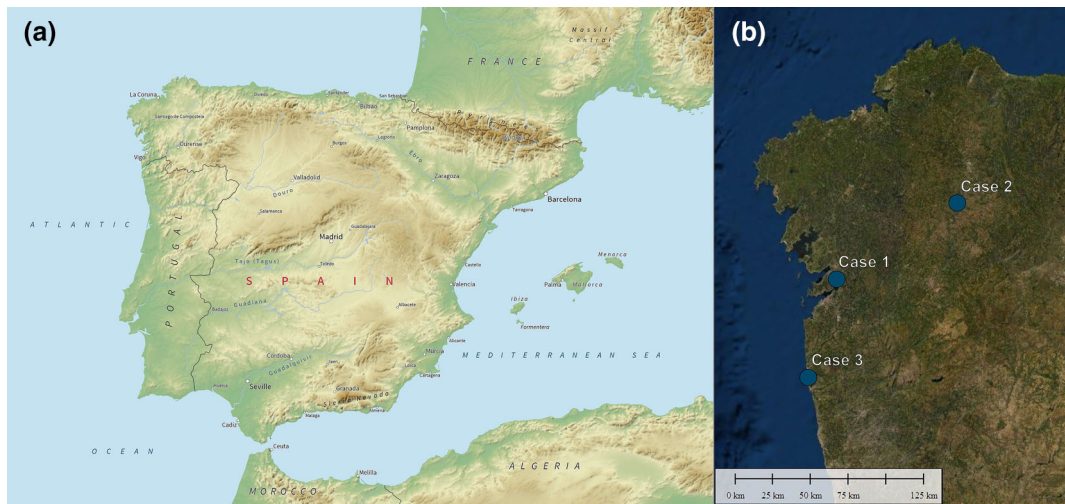


**FIGURE 1** (a) Iberian Peninsula. (b) Galicia and NW Portugal. [Colour figure can be viewed at [wileyonlinelibrary.com](http://wileyonlinelibrary.com)]

Ría (a type of fiord) in Pontevedra, Spain. Located in the intertidal zone of the Ulló marshes, a location favourable for this type of structure, the remains of a tide mill are preserved, as well as the currently named Ulló saline. The salt flats were built in 1637 during the reign of Felipe IV (Méndez et al., 2000) and were abandoned in the 18th century when some of them were converted for agrarian production. Remains of this complex, including a dike with a north–south orientation that isolates the salt flats from the sea (Calo-Lourido, 1997), are still present on the landscape. The tide mill was built in the 19th century to take advantage of the tidal forces caused by the salt dam. Currently, only the foundations of the dike on which the complex was built remain, but these vestiges are important due to the few available examples of these features. The cultural complex, together with the marsh, which is a natural habitat for birds, constitutes a region of incalculable ecological and cultural value. The area was recovered as a walking area in 2006. The works are included in the ‘Salinas do Ulló’ project, which promotes cooperation for the transfer of scientific knowledge regarding cultural landscapes. The intent is to enhance the value of the Vilaboa Salt landscapes as a heritage asset, although the project itself was conceived as a way to leverage cultural resources to promote sustainable and quality tourism. Furthermore, the project is intended to reinforce the maritime identity and social cohesion of the coastal communities. Among the most important actions taken to preserve the value of this heritage site is to develop a graphic and geometric record of the feature and monitor its conservation status. For this purpose, UAVs conducted surveys of the intertidal zone and the salt flats, and a general 3D record of the tide mill was developed.

### 2.1.2 | Case 2. Portomarín Fisheries, Portomarín, Spain

Fisheries may be small dikes or dams built across the course of a river. They may be V- or W-shaped and are positioned where

people fish or channel water to fish. Fisheries are a traditional hydraulic construction, are sometimes complex with weirs, and are generally located in a shallow place or a rocky outcrop where it is possible to fish for lamprey, salmon and other fish species. Minho fisheries were documented in the 12th century, but some of them probably date back to Roman times (Suárez, 2017). They are found in all Galician rivers, especially the Minho River, and have multiple architectural variants. In 1908, there were approximately 700 of these fisheries throughout only 25 km of the Low Minho River basin (Castro Fernández & López Facal, 2019; Domínguez, 2011; Suárez, 2017).

The architectural details of this type of construction are an essential element of the history of this river. An ethnographic study was carried out to document these features, which included a high-resolution geometric registration of 3.2 km of the Minho River near the old town of Portomarín, which was flooded after the construction of the Belesar Reservoir in 1963 (Figure 2b). In addition to multiple fisheries in the area, there are different hydraulic constructions (a mill and power plant) and the remains of an ancient Roman bridge (García et al., 2013; Suárez, 2017). In this case, UAV surveys of the course of the river will be performed during the time of the lowest flow to record the largest possible area. This is in addition to obtaining 3D records and detailed plans of the state of conservation of the existing heritage structures along a 3.2-km stretch that contains fisheries, weirs or archaeological remains.

### 2.1.3 | Case 3. Fornelos engraving. Viana do Castelo, Portugal

Case 3 was a rock art engraving located in the parish of Carreço, Viana do Castelo, Portugal, in an area along the Atlantic coastline. The engraving was found on the pocket beach of Fornelos, on a coastal cliff that is difficult to access (Figure 2c). The first ‘sketch’ of the carvings was performed by Lanhas (1969), but the first tracing

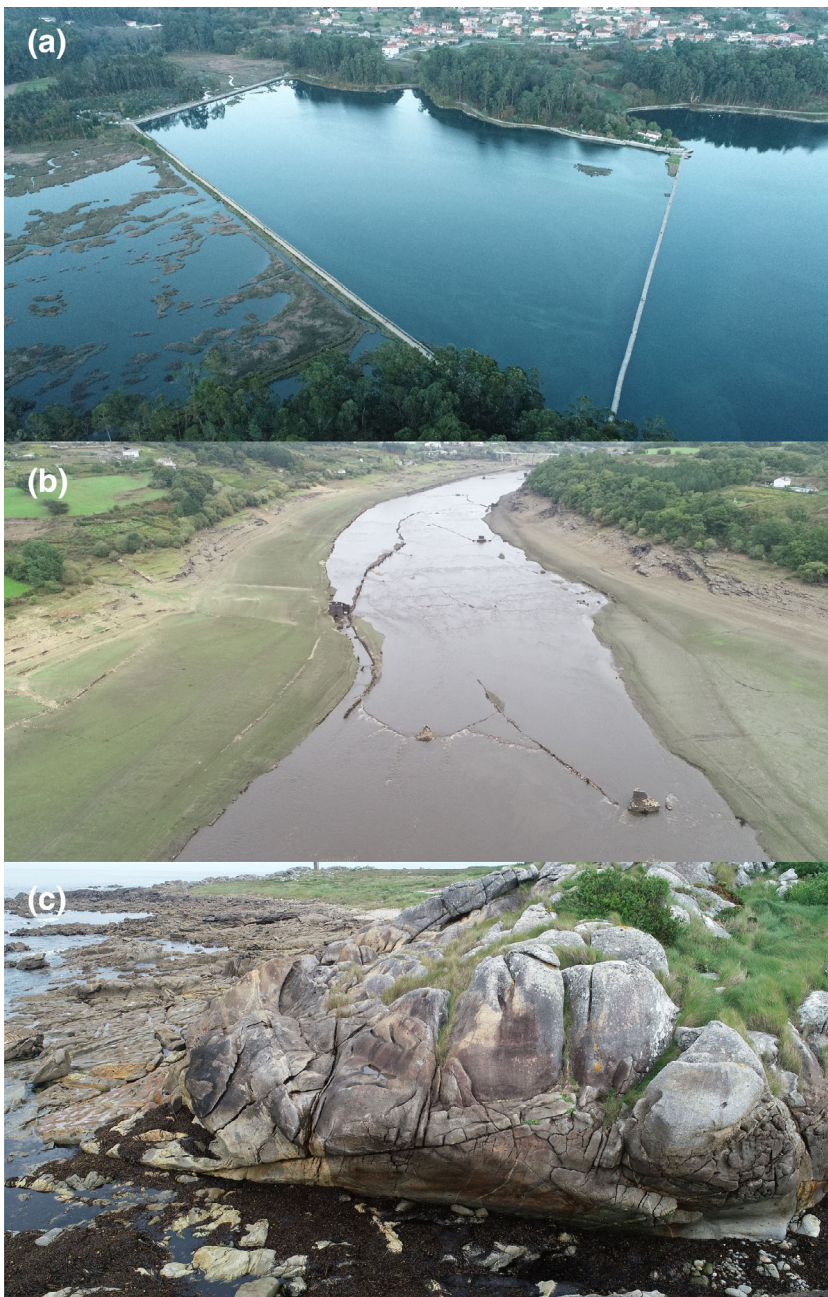


**FIGURE 2** (a) Case 1. Ulló saline. (b) Case 2. Portomarín fisheries. (c) Case 3. Fornelos engraving. [Colour figure can be viewed at [wileyonlinelibrary.com](https://onlinelibrary.wiley.com/doi/10.1002/arp.1901)]

of the carvings was not made until the 1980s, which were considered to have an affinity with the schematic and semi-naturalistic paintings (Baptista, 1986; Baptista & Magalhães, 1985); interpretations were also made by Bradley and Fábregas-Valcarce (1998) and Bradley and Valcarce (1999). New records were subsequently made (Bettencourt, Abad-Vidal, & Rodrigues, 2017; Bettencourt, Silva, et al., 2017), which divided the motifs into three different panels. These panels described various equines, horsemen, a dog and an anthropomorph. Considering these motifs and the interaction between the engraving and the features of the outcrop, it is likely that the images tell a real or mythical narrative. Previous researchers also defended the interpretation that the space chosen for the carving of these images, the orientation of the motifs, the topography of

the outcrop and its colouration create an impressive scenic effect for the audience (Bettencourt, Santos Estevez, et al., 2017; Bettencourt, Silva, et al., 2017). Based on this new interpretation, and because the engravings are increasingly eroded by wind and wave action and are in danger of disappearing, it became necessary to conduct a 3D survey with UAVs and SfM-MVS photogrammetry of the entire south face of the outcrop to better understand the relationship between the motifs and their physical characteristics. The place was classified as Property of Public Interest in the Official Gazette of Portugal by Decree No. 26-A/92, DR, 1st series-B, No. 126 on 1 June 1992, and currently, the location is part of a hiking route, PR7, and is the responsibility of the Municipality of Viana do Castelo.

## 2.2 | Field work

The standard field work for 3D modelling of heritage elements using both aerial and terrestrial photogrammetry consists of two basic tasks. First, an orientation and/or scaling system is established; and second, the photography is planned and executed. In regard to setting up a scaling system, there are two main methods. Scaling of the scene can be accomplished through reference measurements or by establishing a network of ground control points (GCPs) with known coordinates, which also allows the model to be oriented along the XYZ axes. In the case of scaling by reference, this orientation must also be done from a reference such as a plumb line or level for the Z axis to be properly oriented, and a compass is needed to orient the XY axes (Ortiz-Sanz et al., 2010). In inaccessible coastal or river areas, it is not always possible to establish these necessary references, which entails one of the

main difficulties in the geometric registration of cultural heritage located in this type of area.

In all cases, a DJI Phantom IV real-time kinematic (RTK) UAV with a maximum take-off mass (MTOM) of 1.39 kg, a 20-Mpx RGB sensor and a precise positioning module, which ensures centimetric accuracy in image positioning, were used. For flight planning, the GS RTK software that DJI provides with the Phantom IV RTK has been used. The recommended longitudinal and vertical overlaps of 80% and 70%, respectively, were applied. For the measurement of the GCPs, a Stonex S900T GPS RTK was used. Some of the measured points were used as check points (CPs) for independent geometric control (Table 1). Although the techniques and equipment used are common in all the study cases, some particulars are presented below.

### 2.2.1 | Field work in Case 1

This study area covers an area of 28 ha. For the cartographic and topographic survey, a standard photogrammetric flight was carried out at a height of 100 m, which ensures a ground sampling distance (GSD) of 2.75 cm. Figure 3a,b shows photos from these flights. On the other hand, for the survey of linear cultural features, such as the walls of the tide mill dam, oblique flights were made along both sides

**TABLE 1** Field equipment costs.

Field equipment	Cost (\$)	Case
Phantom 4 RTK	5000	All cases
Stonex GPS S900T	5000	Cases 1 and 2
Stonex TS R2 W PLUS	3500	Case 2

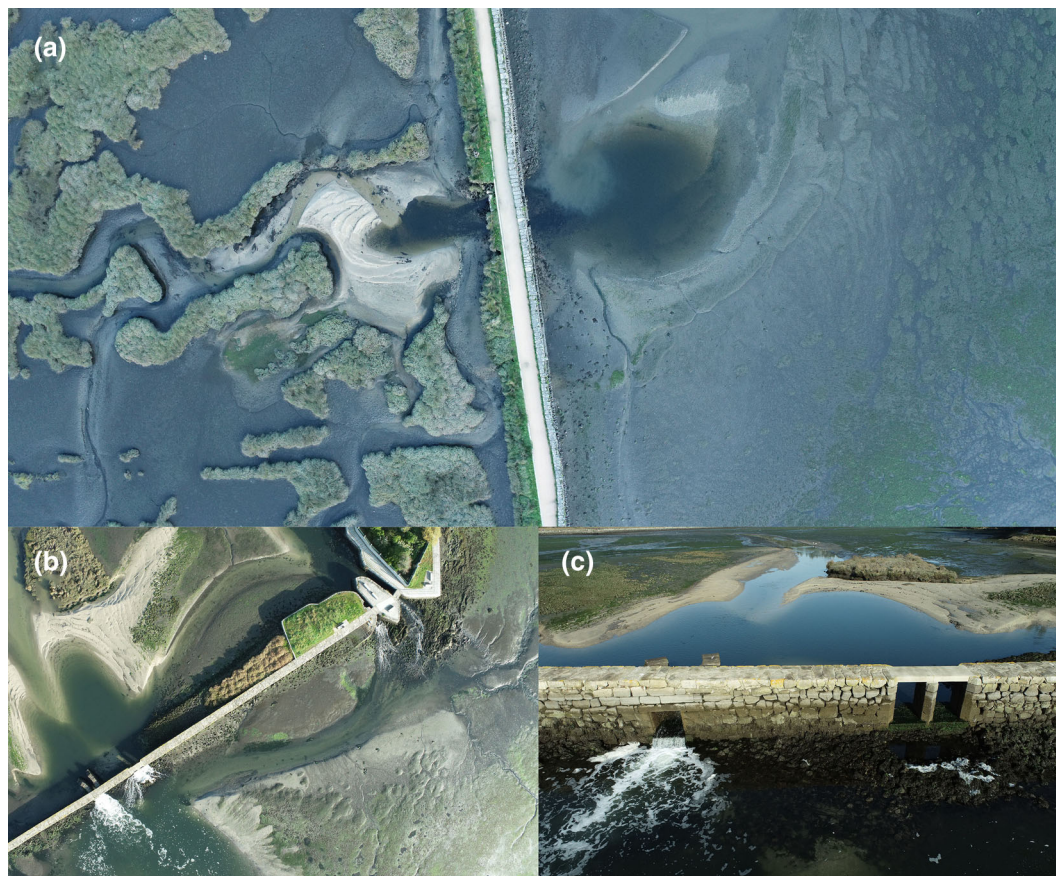


**FIGURE 3** (a) Saline nadiral photo. (b) Tide mill nadiral photo. (c) Tide mill oblique photo. [Colour figure can be viewed at [wileyonlinelibrary.com](https://onlinelibrary.wiley.com)]

of the element to model in detail the vertical walls and construction elements. For this, the camera was configured in automatic shooting mode every 3 s with manual piloting and maintained a constant speed of between 2 and 3 m/s, thus obtaining sufficient overlap. In Figure 3c, an example of an oblique image is shown. Regarding the measurement of GCPs, note that both the sides of the study area and the salt mine dam are easily accessible on foot, so it was possible to establish a network of GCPs with sufficient coverage.

## 2.2.2 | Field work in Case 2

The study occupies an area of 170 ha. As in the previous case, a standard photogrammetric flight at a height of 120 m, which ensures

a GSD of 3.3 cm, was carried out for cartographic and topographic surveys (Figure 4a). For the survey of linear cultural features, as in the previous case, manual oblique flights were conducted with an imaging interval of 3 s. Because of the amplitude of the study area and the large number of survey elements that were often not accessible, it was necessary to carry out flights beyond visual line of sight (BVLOS). First, to locate the buildings (Figure 4d), and second, to obtain enough images to allow a detailed geometric record of specific buildings such as fisheries or mills (Figure 4b,c,e). To do this, several passes were planned at different heights around the elements of interest. In this case, it was difficult to establish the GCP network due to the presence of large, inaccessible areas. To reinforce the georeferencing of the construction elements, a *Stonex R2W Plus* total station (TS) was used to collect laser measurements, which

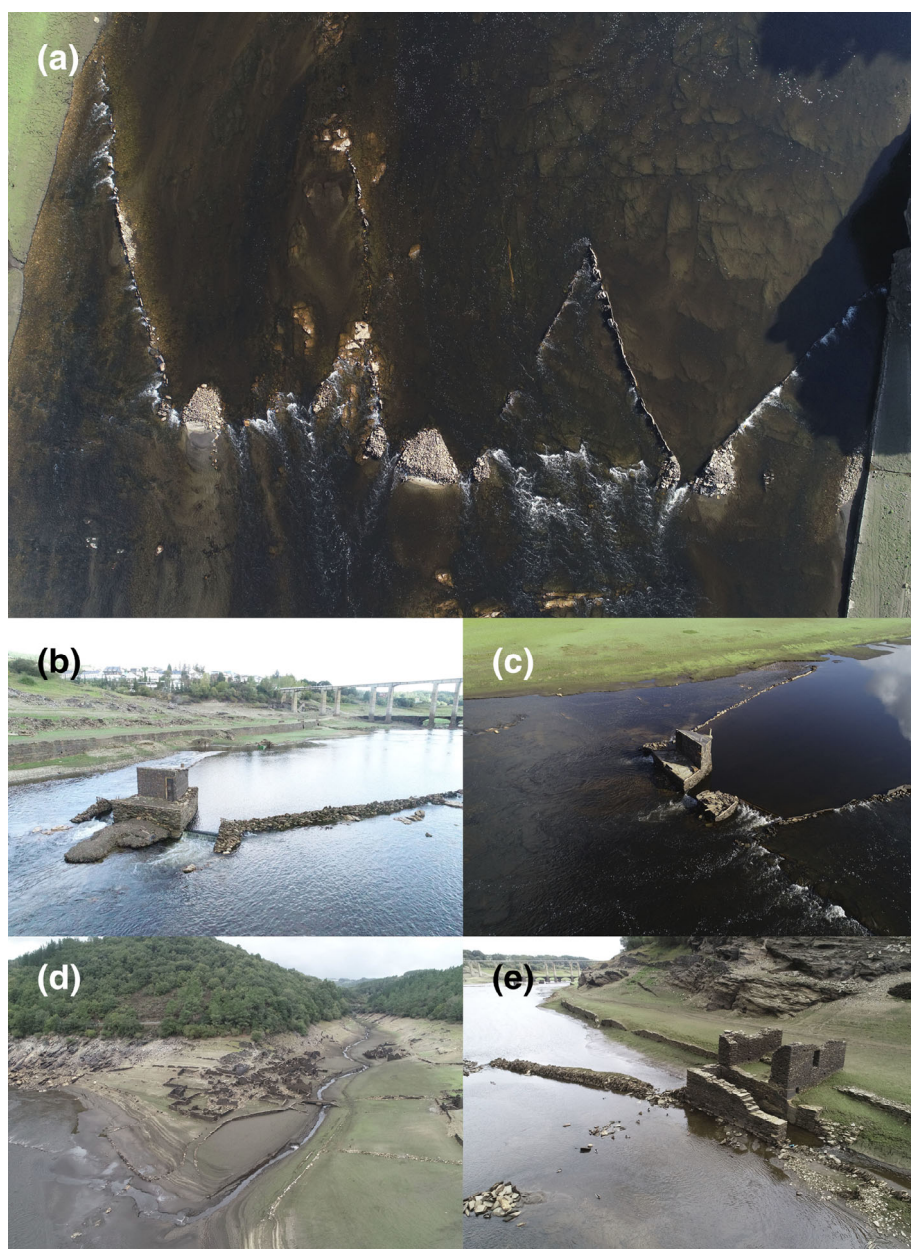


**FIGURE 4** (a) Nadiral photo. (b–e) Oblique photos. [Colour figure can be viewed at [wileyonlinelibrary.com](https://onlinelibrary.wiley.com/terms-and-conditions)]

made it possible to measure the coordinates of various points along these inaccessible features. The rest of the GCPs were measured with the *Stonex S900T* GPS.

### 2.2.3 | Field work in Case 3

The third case study relates to the use of a UAV to photograph a recorded outcrop to elaborate its photogrammetry. Figure 5a shows a general photo of the outcrop, and Figure 5b shows a detailed photo of the engraved panels. The flight was carried out in manual mode without planning for autonomous flight, and a photographic arrangement was applied that was similar to those used with terrestrial cameras often used in this type of work (Gil-Docampo et al., 2019).

## 2.3 | Processing, export and publication

For 3D model processing, *Agisoft Metashape* (Agisoft LLC, Russia) photogrammetric software was used, whereas the enhancement and rendering of the engraving were made possible with *MeshLab* (Visual Computing Lab, ISTI - CNR, Pisa, Italy). In all cases, the three main

steps of the SfM-MVS process were carried out. First, the internal and external orientations of the images were determined. Second, an enhanced-density point cloud was obtained. Both processing phases were carried out at high quality so that the software could use the original image resolution for the process. This technique guarantees the best precision for the photogrammetric adjustment of the cameras and the reconstruction of the point cloud. In both cases, the zenithal and oblique images were processed in individual chunks. Then, 3D models, DEMs, nadiral and side-view orthomosaics, and planimetric vectorizations were merged.

The latest versions of *Agisoft Metashape* incorporate a new mesh generation mode based on depth maps instead of processing from the point cloud (Verhoeven et al., 2021). This mode was used

**TABLE 2** Processing costs.

Software	Cost (\$)
Agisoft Metashape	4000
MeshLab	Free
Workstation Intel(R) Core (TM) i9-9960X CPU @ 3.10 GHz NVIDIA GeForce RTX 2080 Ti	4000



**FIGURE 5** (a) General photo of the outcrop. (b) Detailed photo of the engraved panels. [Colour figure can be viewed at [wileyonlinelibrary.com](https://onlinelibrary.wiley.com)]

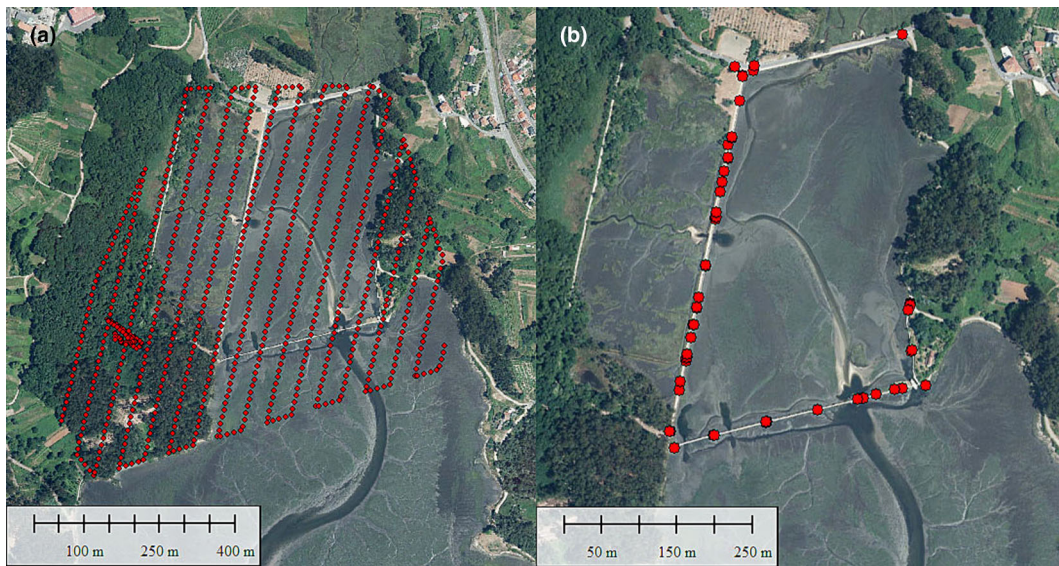


**FIGURE 6** Case 1 (a) Location of the photographic shots. (b) Location of ground control points (GCPs). [Colour figure can be viewed at [wileyonlinelibrary.com](http://wileyonlinelibrary.com)]

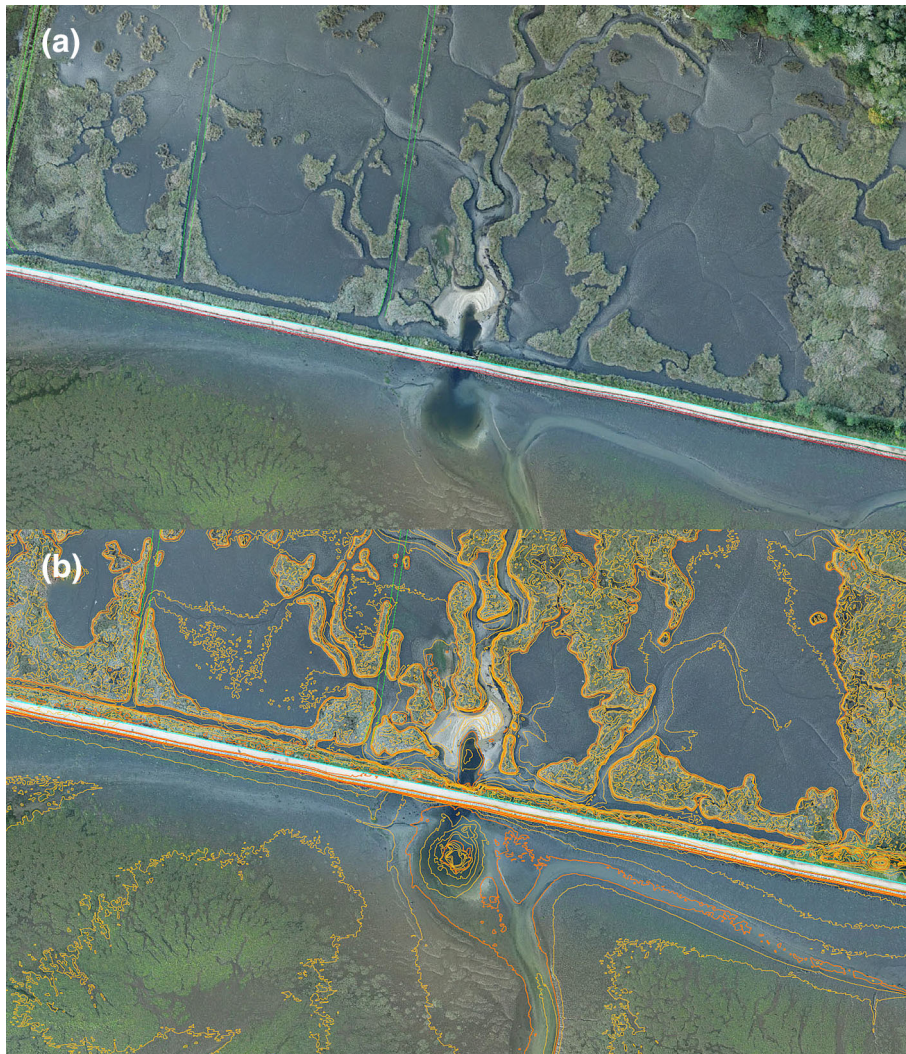


**FIGURE 7** Orthophoto of the salt water inlet and outlet area. [Colour figure can be viewed at [wileyonlinelibrary.com](http://wileyonlinelibrary.com)]



to process oblique images and minimize the noise in areas with water. The same approach was used in Case 3, which consists only of oblique photos, to obtain a better definition from the engraving. Table 2 shows the cost of the software and hardware used to process the three cases.

To publish the results on the SketchFab platform (which actually limits model uploads to 100 MB with the free subscription), the size of the mesh must be reduced. Subsequently, and in all cases, the mesh was exported in Wavefront (obj) format, and the texture file was exported in JPG format and uploaded to the online platform in compressed ZIP format. On the SketchFab platform, an enhancement render was configured to improve the visualization of the results.

### 3 | RESULTS

The results generated in the three case studies are shown below.

#### 3.1 | Case 1. Tide mill and Ulló saline.

In Case 1, a total of 3440 images were obtained, including 846 nadiral and 2594 oblique photos. In this case, 76 points were measured, of which 67 were used as GCPs and 9 as CPs. The work lasted 8 h and was conducted by two people. Figure 6 shows the location of the photographic shots (Figure 6a) and the GCPs (Figure 6b).

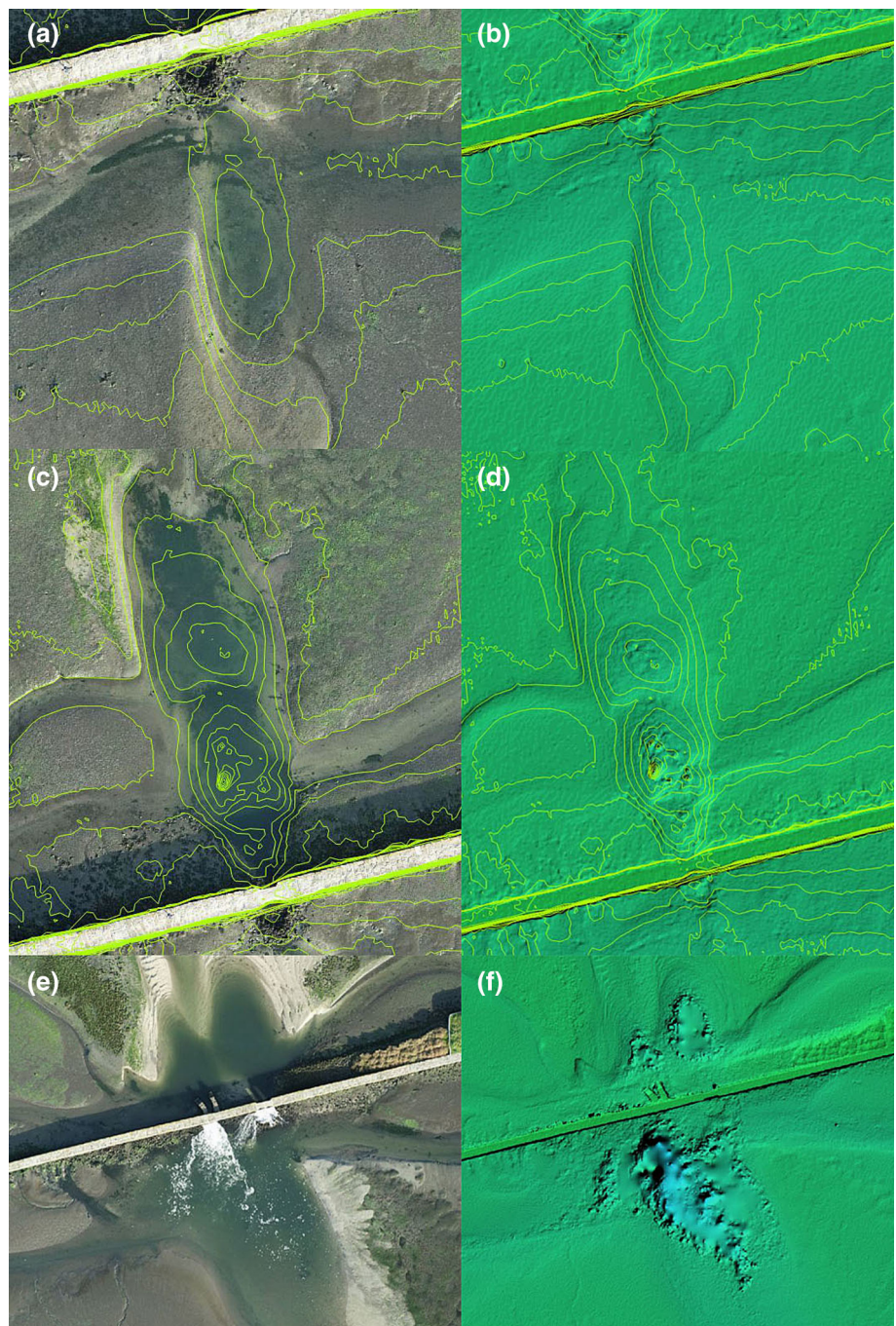


**FIGURE 8** Contours (20 cm) in areas with the presence of water on orthophotos and digital elevation models (DEMs). (a) Area with good results. (b) Area with rectifiable errors. (c) Area with invalid results. [Colour figure can be viewed at [wileyonlinelibrary.com](https://onlinelibrary.wiley.com)]

### 3.1.1 | Ulló saline

Figure 7 shows the orthophoto (Figure 7a) and the topographic contours (Figure 7b) obtained from the salt water inlet and outlet areas.

Figure 8 shows the topographic contours overlain on the orthophoto and the DEM for an area where it was possible to obtain reliable information despite being underwater. Additionally, an area where the foam generated a result with slight errors that could be corrected by debugging the point cloud is also shown. Finally, Figure 8 shows an area where the foam generated invalid results, which made it necessary to complement the topographic record with other techniques or through interpolation.

### 3.1.2 | Tide mill

Figure 9a shows the 3D mesh obtained over one of the mill structures, and Figure 9b shows an orthophoto obtained from the area where the tide mill is located.

## 3.2 | Case 2. Fisheries and weirs

In Case 2, a total of 7341 images were obtained during the flights, which consisted of 1698 nadiral photos and 5643 oblique photos. In

this case, 380 points were measured, of which 357 were used as GCPs and 23 as CPs. The field work lasted 3 days and involved the participation of three people. Figure 10 shows the location of the photographic shots (Figure 10a) and the GCPs (Figure 10b).

The planimetric vectorization of several fisheries and the topographic contours overlain on the orthophoto obtained over a section of the river in Case 2 are shown in Figure 11.

Figure 12 shows a planimetric digitalization (Figure 12a) obtained over one of the fisheries (red shape in Figure 11), as well as its detailed orthophoto (Figure 12b,c) and the side view (Figure 12d,e) of the weirs. Figure 12b shows an orthophoto obtained on a cloudy day, which results in a more homogeneous colour without shadows. On the other hand, orthophoto of Figure 12c was obtained on a sunny day; although shadows can be seen in the image, these are the ideal conditions to obtain seabed information. Figure 12f,g shows the errors produced by the reflections on the surface of the water that caused the structures to be duplicated in the mesh.

## 3.3 | Case 3. Petroglyph and engravings

In Case 3, 223 images of the panel and adjoining rocks were collected. The fieldwork lasted 20 min. The monochrome 3D mesh (Figure 13a) and the photorealistic textured 3D mesh (Figure 13b) obtained in

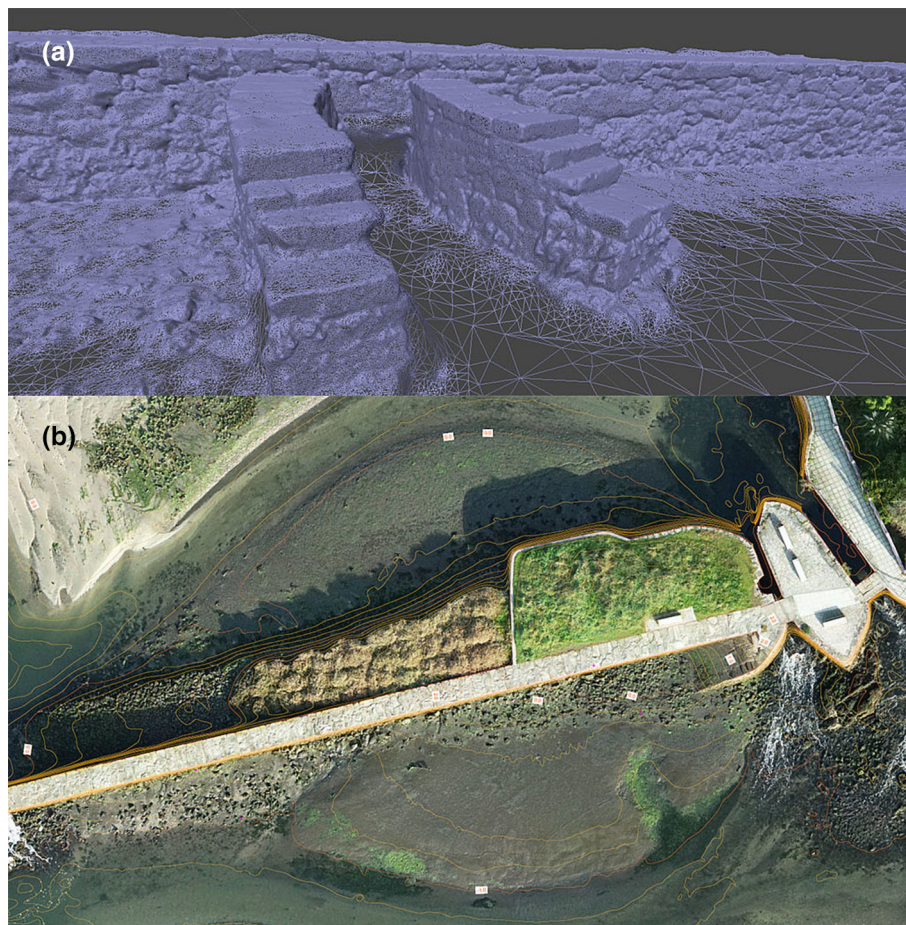


**FIGURE 9** (a) Tide mill structure mesh. (b) Orthophoto of the tide mill area. [Colour figure can be viewed at [wileyonlinelibrary.com](http://wileyonlinelibrary.com)]

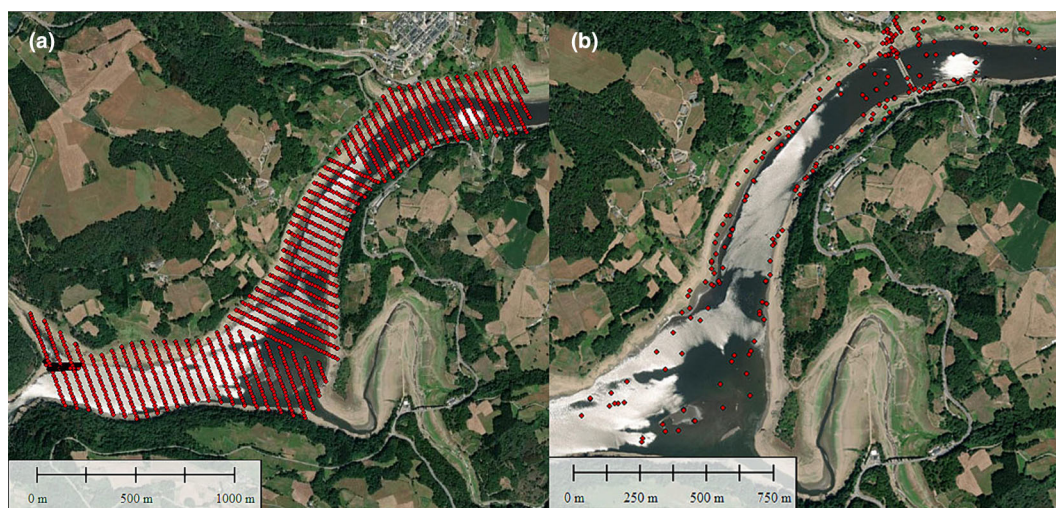


**FIGURE 10** Case 2. (a) Location of the photographic shots. (b) Location of ground control points (GCPs). [Colour figure can be viewed at [wileyonlinelibrary.com](https://onlinelibrary.wiley.com/doi/10.1002/arp.1901)]

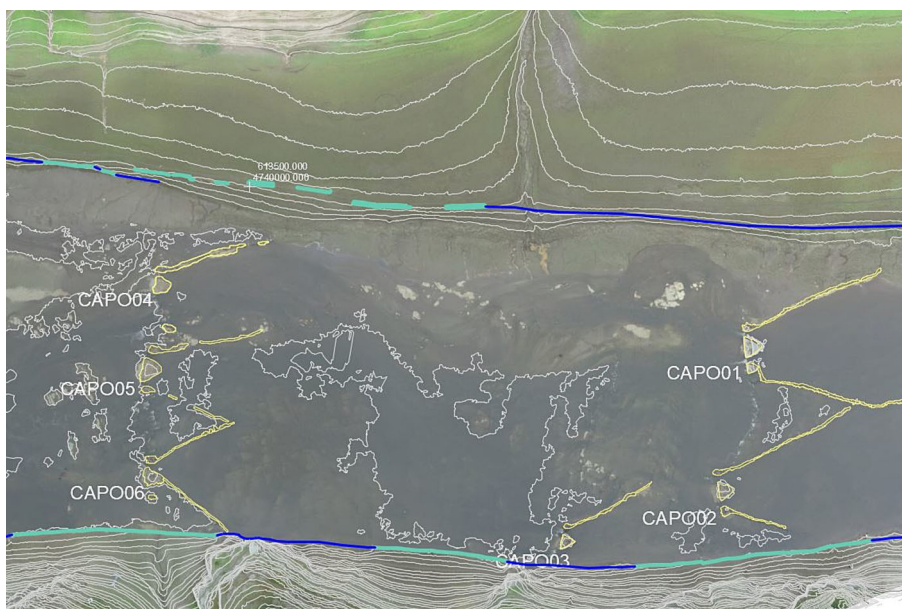


**FIGURE 11** Orthophoto of a river section where six fisheries are observed. [Colour figure can be viewed at [wileyonlinelibrary.com](https://onlinelibrary.wiley.com/doi/10.1002/arp.1901)]

Case 3 are shown below. Figure 13c,d shows the results obtained after the enhanced renderings were applied to the 3D mesh of the rock art.

Case 5: Rock art engraving (RGB): <https://skfb.ly/oyZsW>

Case 6: Rock art engraving (Matcap): <https://skfb.ly/oyZsY>

### 3.4 | Online publication

It is possible to view, download or share the published 3D models from the following links:

Case 1: Ulló saline: <https://skfb.ly/oyZsQ>

Case 2: Fisheries 1: <https://skfb.ly/oyZsT>

Case 3: Fisheries 2: <https://skfb.ly/oyZsU>

Case 4: Roman bridge: <https://skfb.ly/oyZsV>

## 4 | DISCUSSION

Tables 3, 4 and 5 show the results of several examples of the successful application of SfM-MVS photogrammetry combined with UAV, which demonstrates its usefulness as an accurate and cost-effective method for prospecting, surveying, and documenting cultural heritage in coastal or shallow aquatic environments.

The results obtained in Case 1 show that it is possible to obtain a digital terrain model of an intertidal zone using these technologies in an economical and efficient way. Although the initial objective of the

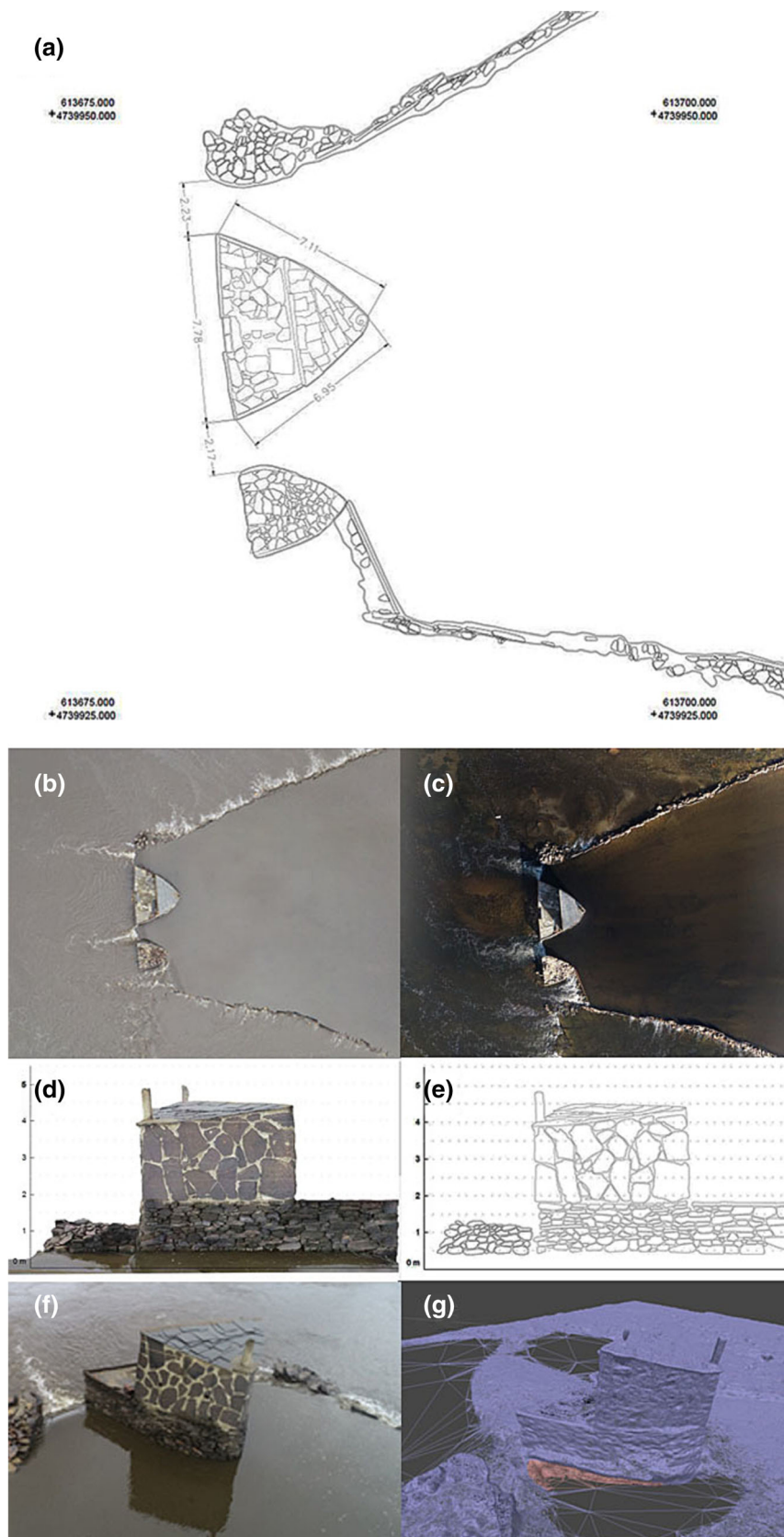


**FIGURE 12** (a) Fishery planimetric digitalization. (b) Detailed orthophoto obtained on a cloudy day. (c) Detailed orthophoto obtained on a sunny day. (d) Orthophoto of the side view of a weir. (e) Planimetric digitalization of the side view. (f) Photo with reflection. (g) Duplication in the mesh. [Colour figure can be viewed at [wileyonlinelibrary.com](http://wileyonlinelibrary.com)]

work was to document only the terrestrial areas, the flights conducted during low tide demonstrated the ability to capture information from the seabed despite the presence of water between 0.5 and 2 m deep.

This allowed the recording of the topography of the intertidal zone of Case 1 with almost complete coverage and with an acceptable level of confidence. For this, aspects such as the turbidity and stillness of the

**FIGURE 13** (a) Monochrome mesh of the outcrop. (b) Photorealistic textured mesh of the engraved outcrop. (c) MatCap rendering in the Sketchfab platform. (d) Radiance scaling rendered in Meshlab software. [Colour figure can be viewed at [wileyonlinelibrary.com](https://onlinelibrary.wiley.com/doi/10.1002/arp.1901)]

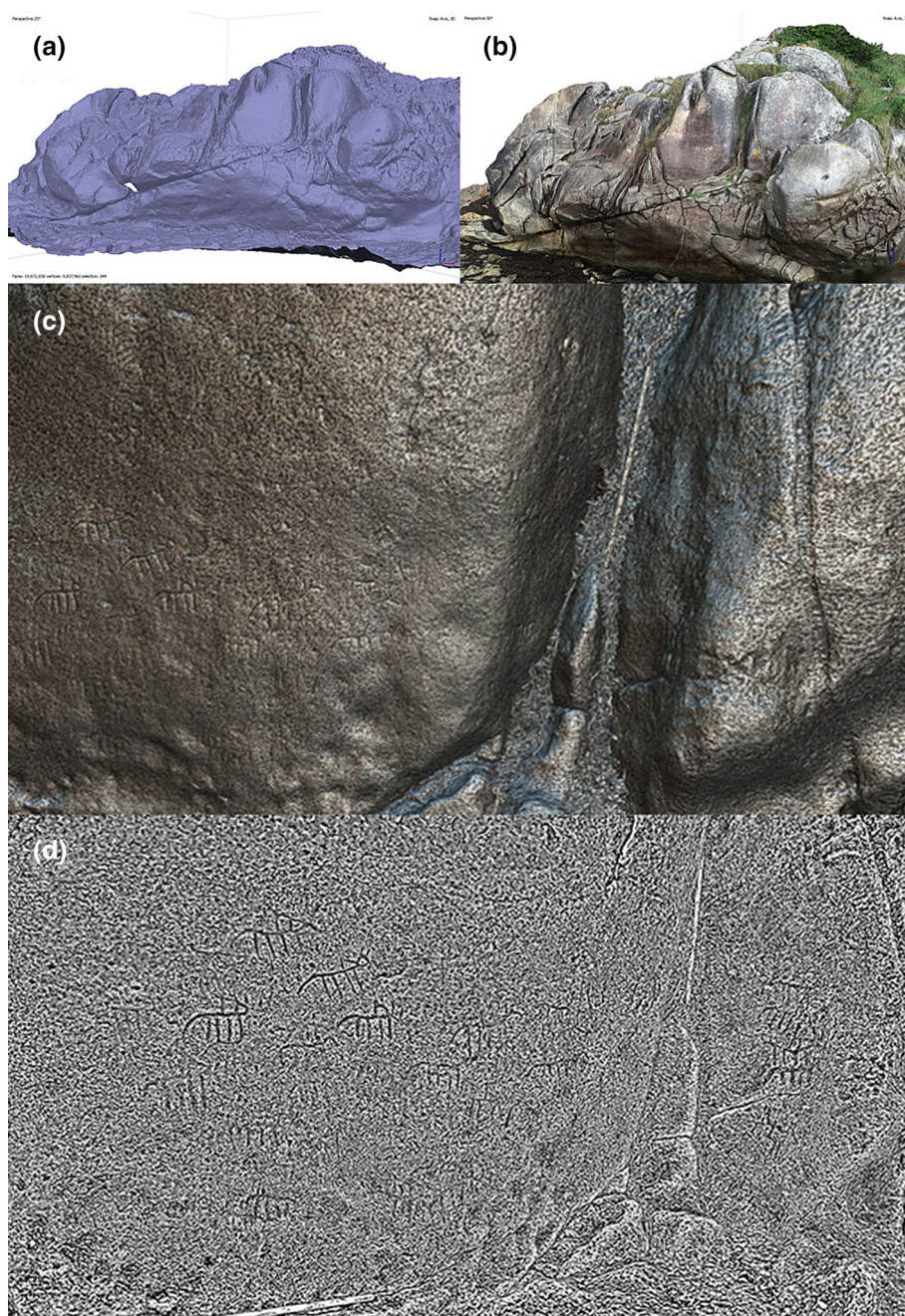


**TABLE 3** Field and processing work information.

Case	Nadiral photos	Oblique photos	GCPs	CPs	GCPs RMS (cm)	CPs RMS (cm)
Case 1	846	2594	67	9	2.06	8.20
Case 2	1698	5643	357	23	3.83	6.14
Case 3	0	223	0	0	-	-

Abbreviations: CPs, check points; GCPs, ground control points.

water, the presence of artefacts, and the texture and characteristics of the seabed are relevant. Under favourable conditions, it is possible to obtain the most information from the bottom. However, a specific analysis would be convenient to contrast the altimetric and planimetric precision of this information. On the other hand, invalid results

with very noisy point clouds are obtained in areas with turbulence, materials floating on the surface, and roughness on the surface of the water due to the effect of the wind or other alterations of the aquatic environment. In these areas, it would be necessary to complement the study with bathymetric methods.

**TABLE 4** Time and cost analysis.

Case	Extension	Field work	Equipment	Equipment and software costs (\$)	Processing time
Case 1	28 ha	1 day × 2 people	UAV, GPS, Metashape, workstation	18.000	16 h
Case 2	170 ha	3 days × 3 people	UAV, GPS, TS, Metashape, workstation	21.500	26 h
Case 3	24 m <sup>2</sup>	20 min × 1 person	UAV, Metashape, workstation	12.000	1 h

Abbreviations: TS, total station; UAV, unmanned aerial vehicle.

**TABLE 5** Exported results.

Case	Nadiral orthophoto	Side views orthophotos	DEM	Detailed 3D models	Detail vectorization	Engraving enhancement render	Online publication
Case 1	X	X	X	Tide mill			X
Case 2	X	X	X	Booths/Roman bridge	X		X
Case 3				X		X	X

Abbreviation: DEM, digital elevation model.

In Case 2, it was observed that flying on a sunny day and taking oblique photos in the opposite direction of the sun is the most effective solution. Although errors due to the effects of water are also common in this case, the topographical and geometric survey allowed for the complete cataloguing of all the fisheries located in this area, many of which were not previously registered and whose location and state of conservation were unknown. However, it would also be necessary to conduct a bathymetric survey of the river's axis. Another technical particularity used in Case 2 that should be highlighted was the measurement of GCPs by combining GPS and TS measurements. This allowed us to optimize the measurement of GCP and improve the photogrammetric adjustment in this complex and inaccessible aquatic environment.

In addition, it should be noted that in both Cases 1 and 2, numerous oblique photos were used to model the architectural structures and to obtain high-resolution photorealistic textured views of the front that allowed detailed plans to be made. Although this represents the largest workload among those two cases, it is of great interest because, for example, the detailed record of the walls that make up the fisheries in Case 2 allows us to analyse the chronological sequence of its construction and complements the ethnographic study, within which the geometric record is included. It is also beneficial because these results handily provide data to disseminate in an informative format.

Regarding the results of Case 3, it should be noted that despite the state of conservation of the engravings, which are highly eroded and hardly noticeable, it was possible to obtain a 3D model of the outcrop with sufficient geometric quality to complete the detection and geometric registration. In this case, the survey was complemented with techniques to enhance rock art engravings to ensure a complete and detailed study, which illustrates quite well the narrative proposed by Bettencourt, Santos Estevez, et al. (2017) and Bettencourt, Silva, et al. (2017) while keeping the outcrop features and motifs in mind. In addition to providing a product of great interest for the study and dissemination of this type of heritage, the methodological flow used is

useful for documenting engravings on cliffs or coastal areas that have not been surveyed because of difficulties in their access; therefore, there may be foreseeable benefits for unpublished rock art. This type of panel with various orientations demonstrates the advantage of studies that have 3D support (e.g., online publications), for which it is possible to study all the detailed elements. This is different from 2D data presentation formats, in which it is not possible to reflect all the detailed elements due to their different orientations.

## 5 | CONCLUSIONS

In all cases, the combination of photogrammetry and UAVs was shown to be a highly efficient technique. This allowed for high-resolution orthophotos, digital terrain models, and topographic contours to be obtained at different levels of detail, which could be applied to the planimetric vectorization or textured 3D models in order to enhance renderings for detailed study or the dissemination of cultural heritage information.

In addition, this work shows that, through close-range photos taken with a commercial UAV, it is possible to document in detail the archaeological structures that may be located in these areas. These structures include tide mills, salt pans or fisheries, which may have limited access, which means that the exclusive use of terrestrial survey techniques may be hindered.

Cases 1 and 2 show that through aerial photogrammetry with a UAV, it is possible to obtain altimetric and planimetric information over shallow aquatic environments. Although the results obtained in both cases are very useful, the experience made it possible to verify the difficulties that aquatic environments present in obtaining quality images for 3D modelling using these techniques. Despite these difficulties, when conditions are optimal (i.e., calm waters or when there is no reflection from the sun that causes glare in the photographs and the wind does not cause waves that prevent the bottom from being seen), the photogrammetric UAV survey works adequately up to a

depth of approximately 2 m. An inconvenience that arises from taking data from the bottom of the water by means of a UAV is the wind-driven roughness of the water and the reflections caused by the angle of the sun on the water. In such circumstances, it is not possible to obtain information because the bottom cannot be imaged. This can be partially solved by stereoscopy point measurements in some areas, and in cases where the angle of the sun causes reflections, slightly oblique flights can be made to the north. On the other hand, in the case of waves created by the wind in the water, a low-pass filter can be used that reduces sharpness and minimizes the effect of surface roughness. This would, in some cases, help obtain more information on bottoms that display distinct bottom features, which would be more easily identified by the software used. Other low-cost bathymetric recording options could be interesting as well, to complement the topography of the areas omitted because of water effects. It would be appropriate to carry out an independent study evaluating all these aspects with precision.

With respect to the UAV, other cheaper models may be valid to obtain similar results in Case 3, which is likely to significantly reduce the cost of the operation. The same does not occur in Cases 1 and 2, where the possibility of having a UAV with RTK positioning is necessary to obtain reliable cartographic information because they are extensive areas where it is not possible to have homogeneous GCPs. In Case 3, it is even possible to use free software for processing because it does not require the generation of cartographic products, as in Cases 1 and 2, where commercial software is necessary.

In addition, this study showed that with a low-cost drone and the application of photogrammetry, it is possible to obtain technical information in a three-dimensional format that can be spread via web media, thus generating an accessible product. The online repository provides viewing, downloading or interaction metrics for statistical tracking. Numerous specialists can study these archaeological sites in detail without accessing them in situ, which may give rise to new hypotheses or help clarify aspects of their construction.

## CONFLICT OF INTEREST STATEMENT

The authors declare no conflict of interest.

## DATA AVAILABILITY STATEMENT

The data that support the findings of this study are openly available in SketchFab at <https://sketchfab.com/SimonPena/collections/archaeological-prospection-26a8363aa06a40f0bc1c1bb4b0f36cc0/>.

## ORCID

Mariluz Gil-Docampo  <https://orcid.org/0000-0002-9037-9944>

Simón Peña-Villasenín  <https://orcid.org/0000-0002-6297-0358>

## REFERENCES

- Agüera-Vega, F., Carvajal-Ramírez, F., & Martínez-Carricondo, P. (2017). Assessment of photogrammetric mapping accuracy based on variation ground control points number using unmanned aerial vehicle. *Measurement*, 98, 221–227.
- Aicardi, I., Chiabrande, F., Lingua, A. M., & Noardo, F. (2018). Recent trends in cultural heritage 3D survey: The photogrammetric computer vision approach. *Journal of Cultural Heritage*, 32, 257–266.
- Baptista, I. (1986). Arte rupestre de Carreço. *Centro de Estudos Regionais. Boletim Cultural*, 3, 117–128.
- Baptista, I., & Magalhães, C. (1985). Arte rupestre de Carreço. *Centro de Estudos Regionais. Boletim Cultural*, 2, 92–102.
- Bettencourt, A., Abad-Vidal, E., & Rodrigues, A. (2017). CVARN - Rock art virtual corpus of north-western Portugal. A multimedia tool to investigate and describe post-palaeolithic rock art.
- Bettencourt, A., Santos Estevez, M., Sampaio, H. A., & Cardoso, D. (Eds.). (2017). *Recorded places, experienced places: The Holocene rock art of the Iberian Atlantic north-west*. BAR Publishing.
- Bettencourt, A., Silva, I. S., Alves, M. I., Simões, P. P., & Santos Estévez, M. S. (2017). Where do the horses run? A dialogue between signs and matter in the rock carvings of Fornelos (Viana do Castelo, north-west Portugal). In *Recorded places, experienced places: The holocene rock art of the Iberian Atlantic north-west* (pp. 167–177). BAR Publishing. ISBN 978-1-4073-1484-6.
- Bradley, R., & Fábregas-Valcarce, R. (1998). Crossing the border: Contrasting styles of rock art in the prehistory of north-west Iberia. *Oxford Journal of Archaeology*, 17(3), 287–308. <https://doi.org/10.1111/1468-0092.00064>
- Bradley, R., & Valcarce, R. F. (1999). La “ley de la frontera”: Grupos rupestres galaico y esquemático y Prehistoria del Noroeste de la Península Ibérica. *Trabajos de Prehistoria*, 56(1), 103–114.
- Brumana, R., Oreni, D., Cuca, B., Binda, L., Condoleo, P., & Triggiani, M. (2014). Strategy for integrated surveying techniques finalized to interpretive models in a byzantine church, Mesopotam, Albania. *International Journal of Architectural Heritage*, 8(6), 886–924. <https://doi.org/10.1080/15583058.2012.756077>
- Calo-Lourido, F. (1997). NOTAS PARA O ESTUDIO DO SAL EN GALICIA. Periepias dunhas salinas. *Portugalia*, 17, 211.
- Castro Fernández, B., & López Facal, R. (2019). Portomarín: la memoria herida de un desarraigo. *Revista Electrónica Interuniversitaria de Formación Del Profesorado*, 22(2). <https://doi.org/10.6018/reifop.22.2.363841>
- Chandran, V., Carswell, B., Boashash, B., & Elgar, S. (1997). Pattern recognition using invariants defined from higher order spectra: 2-D image inputs. *IEEE Transactions on Image Processing*, 6(5), 703–712. <https://doi.org/10.1109/83.568927>
- Domínguez, A. B. M. (2011). Traslado y reconstrucción de Portomarín. Patrimonio de Galicia [Online Resource]: Arquitecturas a Estudio, 3.
- Dong, Z., Liang, F., Yang, B., Xu, Y., Zang, Y., Li, J., Wang, Y., Dai, W., Fan, H., & Hyyppä, J. (2020). Registration of large-scale terrestrial laser scanner point clouds: A review and benchmark. *ISPRS Journal of Photogrammetry and Remote Sensing*, 163, 327–342.
- Furukawa, Y., Curless, B., Seitz, S. M., & Szeliski, R. (2010). Towards internet-scale multi-view stereo. Proceedings of the IEEE Computer Society Conference on Computer Vision and Pattern Recognition, 1434–1441. <https://doi.org/10.1109/CVPR.2010.5539802>
- Furukawa, Y., & Ponce, J. (2010). Accurate, dense, and robust multiview stereopsis. *IEEE Transactions on Pattern Analysis and Machine Intelligence*, 32(8), 1362–1376. <https://doi.org/10.1109/TPAMI.2009.161>
- García, M. D. D., Horlings, L., Swagemakers, P., & Fernández, X. S. (2013). Place branding and endogenous rural development. Departure points for developing an inner brand of the River Minho estuary. *Place Branding and Public Diplomacy*, 9(2), 124.
- Gil-Docampo, M., Peña-Villasenín, S., & Ortiz-Sanz, J. (2019). An accessible, agile and low-cost workflow for 3D virtual analysis and automatic vector tracing of engravings: Atlantic rock art analysis. *Archaeological Prospection*, September, 2020, 1–16. <https://doi.org/10.1002/arp.1760>
- Guarnieri, A., Milan, N., & Vettore, A. (2013). Monitoring of complex structure for structural control using terrestrial laser scanning (TLS) and

- photogrammetry. *International Journal of Architectural Heritage*, 7, 54–67. <https://doi.org/10.1080/15583058.2011.606595>
- Heincke, B., Jackisch, R., Saartenoja, A., Salmirinne, H., Rapp, S., Zimmermann, R., Pirttijärvi, M., Vest Sörensen, E., Gloaguen, R., Ek, L., Bergström, J., Karinen, A., Salehi, S., Madriz, Y., & Middleton, M. (2019). Developing multi-sensor drones for geological mapping and mineral exploration: Setup and first results from the MULSEDRO project. *Geological Survey of Denmark and Greenland Bulletin*, 43, e2019430302. <https://doi.org/10.34194/GEUSB-201943-03-02>
- Lanhas, F. (1969). As gravuras rupestres de Montedor. *Revista de Etnografia*, 13(2), 367–386.
- Lowe, D. G. (1999). Object recognition from local scale-invariant features. *Iccv*, 99(2), 1150–1157.
- Lowe, G. (2004). SIFT - The scale invariant feature transform. *International Journal*, 2, 91–110.
- Martínez, S., Ortiz, J., Gil, M. L., & Rego, M. T. (2013). Recording complex structures using close range photogrammetry: The cathedral of Santiago de Compostela. *The Photogrammetric Record*, 28(144), 375–395. <https://doi.org/10.1111/phor.12040>
- Méndez, G., Rey, D., Bernabeu, A. M., Manso, F., & Vilas, F. (2000). Recursos minerales marinos en las rías gallegas y en la plataforma continental adyacente. *Journal of Iberian Geology*, 26, 67–97.
- Ortiz-Sanz, J., Gil-Docampo, M. L., Martínez-Rodríguez, S., Rego-Sanmartín, M. T., & Meijide-Cameselle, G. (2013). Three-dimensional modelling of archaeological sites using close-range automatic correlation photogrammetry and low-altitude imagery. *Archaeological Prospection*, 20(3), 205–217. <https://doi.org/10.1002/arp.1457>
- Ortiz-Sanz, J., Gil-Docampo, M. L., Martínez-Rodríguez, S., Sanmartín-Rego, M. T., & Meijide-Cameselle, G. (2010). A simple methodology for recording petroglyphs using low-cost digital image correlation photogrammetry and consumer-grade digital cameras. *Journal of Archaeological Science*, 37(12), 3158–3169. <https://doi.org/10.1016/j.jas.2010.07.017>
- Peña-Villasenín, S., Gil-Docampo, M., & Ortiz-Sanz, J. (2017). 3-D modelling of historic facades using SfM photogrammetry metric documentation of different building types of a historic centre. *International Journal of Architectural Heritage*, 11(2017), 871–890. <https://doi.org/10.1080/15583058.2017.1317884>
- Peña-Villasenín, S., Gil-Docampo, M., & Ortiz-Sanz, J. (2019). Professional SfM and TLS vs a simple SfM photogrammetry for 3D modelling of rock art and radiance scaling shading in engraving detection. *Journal of Cultural Heritage*, 37, 238–246.
- Peña-Villasenín, S., Gil-Docampo, M., & Ortiz-Sanz, J. (2020). Desktop vs cloud computing software for 3D measurement of building façades: The monastery of San Martín Pinarío. *Measurement*, 149, 106984. <https://doi.org/10.1016/j.measurement.2019.106984>
- Pepe, M., & Costantino, D. (2020). Techniques, tools, platforms and algorithms in close range photogrammetry in building 3D model and 2D representation of objects and complex architectures. *Computer-Aided Design and Applications*, 18, 42–65.
- Remondino, F., Barazzetti, L., Nex, F., Scaioni, M., & Sarazzi, D. (2011). UAV photogrammetry for mapping and 3d modeling—Current status and future perspectives. *The International Archives of the Photogrammetry, Remote Sensing and Spatial Information Sciences*, 38(1), C22.
- Remondino, F., & El-Hakim, S. (2006). Image-based 3D modelling: A review. *The Photogrammetric Record*, 21(115), 269–291. <https://doi.org/10.1111/j.1477-9730.2006.00383.x>
- Santagati, C., Inzerillo, L., & Di Paola, F. (2013). Image-based modeling techniques for architectural heritage 3D digitalization: Limits and potentialities. *ISPRS - International Archives of the Photogrammetry, Remote Sensing and Spatial Information Sciences*, XL-5/W2 (September), 555–560. <https://doi.org/10.5194/isprsarchives-XL-5-W2-555-2013>
- Santos-Estevez, M., Tejerizo-García, C., & Toucido, F. A. (2020). El abrigo con pintura esquemática de Pala de Cabras (Ourense). Encuentros y desencuentros entre dos tradiciones. *Complutum*, 31(1), 7–24.
- Snavely, N., Seitz, S., & Szeliski, R. (2006). Photo tourism: Exploring photo collections in 3D. *SIGGRAPH Conference Proceedings*, 835–846. <https://doi.org/10.1145/1141911.1141964>
- Snavely, N., Seitz, S. M., & Szeliski, R. (2008). Modeling the world from internet photo collections. *International Journal of Computer Vision*, 80(2), 189–210. <https://doi.org/10.1007/s11263-007-0107-3>
- Suárez, M. C. (2017). Construcións populares das serras ourensás. *Rai-game: Revista de Arte, Cultura e Tradicións Populares*, 41, 86–101.
- Themistocleous, K. (2020). The use of UAVs for cultural heritage and archaeology. In *Remote sensing for archaeology and cultural landscapes* (pp. 241–269). Springer.
- Verhoeven, G., Santner, M., & Trinks, I. (2021). From 2D (to 3D) to 2.5 D: Not all gridded digital surfaces are created equally. In *28th CIPA Symposium "Great Learning & Digital Emotion"* (Vol. 8, pp. 171–178). <https://doi.org/10.5194/isprs-annals-VIII-M-1-2021-171-2021>
- Westoby, M. J., Brasington, J., Glasser, N. F., Hambrey, M. J., & Reynolds, J. M. (2012). Structure-from-motion photogrammetry: A low-cost, effective tool for geoscience applications. *Geomorphology*, 179, 300–314. <https://doi.org/10.1016/j.geomorph.2012.08.021>

**How to cite this article:** Gil-Docampo, M., Peña-Villasenín, S., Bettencourt, A. M. S., Ortiz-Sanz, J., & Peraleda-Vázquez, S. (2023). 3D geometric survey of cultural heritage by UAV in inaccessible coastal or shallow aquatic environments. *Archaeological Prospection*, 1–16. <https://doi.org/10.1002/arp.1901>